Biol. Cybern. 49, 33–43 (1983)

Biological Cybernetics

Pervasive Locking, Saturation, Asymmetric Rate Sensitivity and Double-Valuedness in Crayfish Stretch Receptors*

O. Diez Martínez**, A. F. Kohn***, and J. P. Segundo

Department of Anatomy and Brain Research Institute, University of California, Los Angeles, CA, USA

Abstract. The correspondence between afferent discharges and sinusoidal length modulations (0.2–10 cps, under 10% of the natural length variations) was studied in isolated fast-adapting stretch receptor organs (FAO) of crayfish, largely using average displays of rate vs. length (or derivatives) along the cycle. Rate modulations were greatest during early cycles and then stabilized, an initial adjustment remindful of mechanical preconditioning. Responses to stimulation in the FAO, as in the slowly-adapting organs (SAO) and possibly other receptors, exhibit the following features, all striking because of their magnitude and ubiquity. i) A zig-zag overall afferent rate vs. stimulus frequency graph with positively and negatively sloped segments. This precludes the straighforward use of Bode plots. ii) Marked non-linearities as an obvious stimulus-response locking in the positively sloped segments, a double-valuedness with one rate while stretching and another while shortening, a lower-limit saturation with the receptor silent for more than half a cycle, and an asymmetric rate sensitivity. iii) Clear-cut discharge leads relative to the stimulus at low frequencies and lags at high ones. The FAO responds worse than the SAO to low frequencies, and better to high ones; it is locked 1-to-1 in a much broader range (e.g., 3–100 vs. 1–3 cps). All features were strongly frequency-dependent. With higher frequencies: i) the number of impulses per cycle fell from several to just one and finally to one every several cycles at higher values; ii) the two values of each length approached one another usually but not always; iii) the silent proportion of the cycle increased; and iv) the rate sensitivity changed. Each feature can arise in principle at any of the transduction stages from length to discharge: the mechanical transduction from length to dendritic deformation, and the encoder one from generator potentials to discharges are particularly likely candidates.

* Supported by funds from the Brain Research Institute and by a scholarship to ODM from the Departamento de Becas, Universidad Nacional Autónoma de México (UNAM) and by a scholarship to AFK from FAPESP (Brasil)

** Present address: Departamento de Fisiología, Fac. de Medicina, UNAM, México DF 04510, México

*** Present address: Esc. Politecnica, DEE, USP Cx. Postal 8174, Sao Paulo, S.P., Brasil

Introduction

This communication describes in fast-adapting stretch receptor organs of crustacea the correspondence between sinusoidal length modulations and afferent discharges, an analysis carried out previously in the slowly adapting organ (Borsellino et al., 1965; Brown and Stein, 1966; Chaplain et al., 1971; Vibert and Segundo, 1979). We stress the importance of non-linearities, striking and ever-present in the natural operational range, as well as their frequency-dependence. The effect of modulation depth and background length will be reported subsequently (Diez Martínez and Segundo, in preparation).

Materials and Methods

Fast-adapting organs (FAO) of Procambarus clarkii of either sex were studied in June, July, and August. Organs were 4–12 mm in length in specimens of 9–14 cm. The procedures for dissecting, mounting in about 14 °C van Harreveld solution, stimulating, recording, and storing data are described elsewhere (Buño et al., 1978; Vibert et al., 1979).

Only the 8th thoracic segment receptors were used. First the physiological range of their length changes was estimated (usually 3.5–4 mm) by observing under the dissecting microscope what happened when the cephalic FAO insertion was fixed and the caudal one displaced by going from extreme abdominal extension to extreme flexion. After measurement, the caudal end, inserted to the tergum of the first abdominal segment,

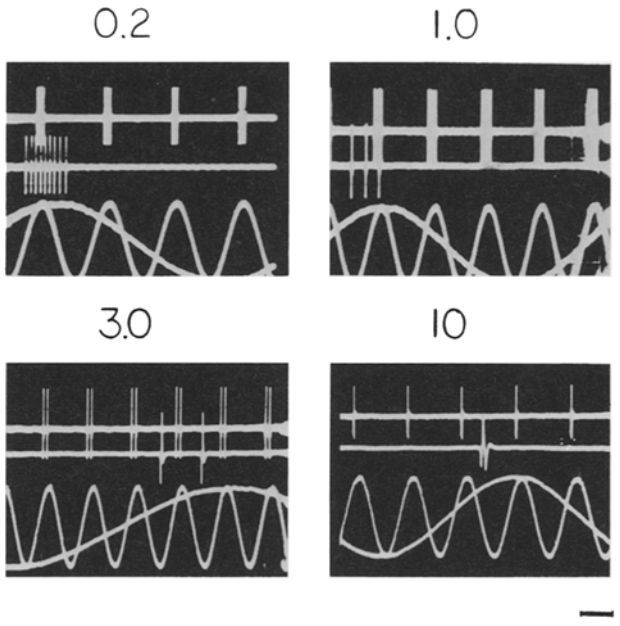

Fig. 1. Effect of stimulus frequency upon spike discharge: The discharge responded to the stimulus by a modulation at the stimulus frequency, and the number of spikes per cycle decreased as stimulus frequency increased. Cycles chosen randomly from stationary periods. A fast and a slow sweep speed were used for each frequency. (Calibrations: 2 or 0.5 s with 0.2, 0.5 or 0.1 s with 1.0, 0.2 or 0.02 s with 3.0, and 0.050 or 0.010 s with 10 cps.) The uppermost trace is the spike discharge at the slow sweep; the next trace is that for one individual cycle; the length recordings are superimposed at both speeds; modulation depth, 0.24 mm; total receptor length, 5.1 mm

was immobilized by anchoring the latter with a pin to the paraffin. Stimuli consisted in length variations imposed upon the receptor by the movement of a forceps that clamped the organ between its sensory innervation and cephalic insertion, and was attached to a Ling Electronics 102 A electromagnetic shaker, whose input was a sine wave from a Wavetek 132 signal generator. The stretching device followed with periodic, approximately sinusoidal, modulations, measured by a Grass FT0 3C force-displacement transducer. Four frequencies – 0.2, 1.0, 3.0, and 10 cps – were used systematically; others, up to 100 cps, only occasionally. The 0.06–0.75 mm depth of the modulations i.e. peak to peak amplitude), adjusted through the microscope, was roughly 1–10% of total receptor length and 2–20% of its physiological changes. The 0.02–15 mm/s velocities were within physiological ranges also, since escape response extensions reach 30 mm/s (Brown, 1967). The "background" length, i.e., the minimal distance between the caudal insertion and the forceps, was set always to within the natural range. We call "resting" a length corresponding approximately to an intermediate abdominal flexion in the quiescent intact animal.

Primary afferent discharges were recorded extracellularly from the dorsal nerve cut close to the ventral cord. The FAO did not discharge spontaneously, and its spikes were generally larger than those of the SAO; when smaller or similar, interference was avoided by silencing the SAO by freeing or damaging it. Recording at a particular frequency lasted from 10 to 1000 s usually a sample of about 1000 spikes sufficed for statistical analysis, taking longer to collect with lower frequencies and weaker discharges; larger samples (e.g. 5000 spikes) were required for special processing, to observe adaptation, etc. A 10-min between-stimulus interval was allowed to reduce interactions which, though very real, were not analyzed.

Data were stored on analog tape and analyzed subsequently using a PDP-8E DEC computer. The spike trains were divided into adjacent sampling epochs of, say, 1000 ms referred to as "bins." The number of spikes in each bin divided by the bin-width gave the "bin-rate," i.e., the impulse rate in impulses/s (ips) averaged across that bin. Bin-rate was displayed as a function of ongoing time. The first trend-free or stationary segment, i.e., with "fully adapted discharges," was identified testing for the "null hypothesis of no trend" (Kendall, 1970); all tests were at least at a 95% significance level. Cycle histograms were obtained only from stationary segments, selecting bin-widths of 1/10 the average period; other widths were used for gross data examination, or for studying locking and sensitivity. The length variations were changed into trains of impulses at very high rates using a voltage-to-rate converter. Plots of "average bin-rate" or of "average length" in the ordinate vs. time along the cycle in the abscissa were constructed. The rate standard deviations (SD) and coefficients of variation (CV = SD/average) were calculated for each bin. The average number of spikes per cycle and the overall average rate were determined also.

Lissajous figures of discharge intensity vs. stimulus magnitude were constructed displaying the average rate in the ordinate and the corresponding average length in the abscissa. A second Lissajous type displayed intensity vs. velocity, i.e., discharge rate vs. change in length from the previous bin. A third Lissajous plotted intensity vs. acceleration, i.e. discharge rate vs. change in velocity.

The sensitivities of the FAO to length at the different frequencies were compared by using identical modulation depths and bin-widths (of from 10 to 500 ms) at all frequencies; bins greater than half the stimulus period were not used. The minimum-to-peak swing in rate during the average cycle was taken as an index of the sensitivity. Other criteria might lead to different conclusions.

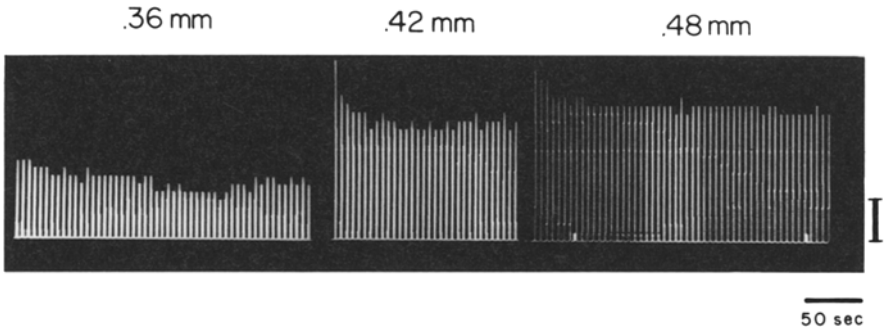

Fig. 2. Periodic length modulation at 0.2 cps. Effect of modulation depth. The receptor responded to the stimulus with a modulation at the same frequency, maximum at the onset and declining to a steady level after several cycles. Bin-rate vs. ongoing time displays. Overall rates increased from 2.17 to 5.14 and to 5.92/s when depth was increased from 0.36 to 0.42 and 0.48 mm, respectively

Results

The afferent discharge was modulated commonly at the same frequency as the stimulus (Fig. 1), showing an across-frequency gradient in practically all its response characteristics. The discharge rate modulation depth (Fig. 2) was greatest along the first cycles and then declined to a steady level. The initial response decline and the time (and number of cycles) it took to settle were greater at the lower frequencies: for example, a decline of 4 ips over 18 s (18 cycles) at 1.0 cps as opposed to 2 ips over 0.5 s (5 cycles) at 10 cps. This behavior at the stimulus onset was not studied systematically; subsequent paragraphs refer only to stationary periods.

The raw records themselves showed that, at a given background length and modulation depth, the number of spikes per cycle decreased with increasing frequency (Fig. 1), being 5–36 for 0.2, 2–7 for 1.0, 1–5 for 3.0, and 1–3 for 10 cps. Figure 3 illustrates that, even with a moderate depth of 0.30 mm, there might be no FAO discharges at the lower frequencies, e.g., 0.2 and 1.0 cps; contrastingly, it usually responded even with small depths (e.g., 0.09 mm) at the higher frequencies. A common response between 3.0 and 100 cps was to have a single spike in every cycle, in which case the stimulus frequency and the overall discharge rate were equal: the position of the spike changed little from cycle to cycle (i.e., there was "one-to-one locking," see later); the impulse preceded the peak length or "led" with 3.0, 10 and 20 cps and followed it or "lagged" with 50 cps or over.

The overall average rate increased with frequency, at given background length and modulation depth (Table 1). Ratios of stimulus frequency to discharge rate (e.g., with a 0.18 mm depth) were, for example, 0.19 for 0.2 cps, 0.29 for 1.0 cps, 0.49 for 3.0 cps, and 1 for 10 cps. The one-to-one locking segment started around 3 cps, always included 10 cps, and extended to 100 cps.

The average Lissajous plots of rate vs. length usually had a flat extension at the minimum lengths and a loop at the maximum ones (Figs. 4C and 5C), but the rate modulation changed with frequency (Figs. 4B and 5B). Usually, loops with 0.2 and 1.0 cps were folium-like; with 3.0 cps, folium-like or triangular with bases against the abscissae; and with 10 cps, triangular with a narrow base. The loop implied that for certain lengths there were two rates (double-valuedness) depending on whether reached by elongation or shortening. The increasing and decreasing segments in the loops usually were concave up and to the left, each with one intermediate bin. In some 3.0 and 10 cps cases (close-to-resting background lengths, depths 0.18–0.75 mm), two or three adjacent bins, including that with the greatest elongation, exhibited identical high rates (e.g., 100 ips with 10 cps), an upper-limit saturation-like phenomenon.

Commonly at all frequencies the rate peaked prior to the length, leading it by about 1 bin (1/10 of the stimulus period); thus loops commonly developed clockwise at all frequencies (Table 2, Figs. 4C and 5C). The clockwise percentage decreased with stimulus frequency, however, from 95% (18/19) at 0.2 cps, through 82% (14/17) at 1.0 cps, and 74% (17/23) at 3.0 cps, to 71% (12/17) at 10 cps. Counter-clockwise loops were observed with 0.2, 1.0, 3.0, and 10 cps in 1/19, 3/17, 6/23, and 5/17 of cases, respectively: the rate lagged the length with 0.2 cps (2 bin lag) and 1.0 cps (1 bin), but usually was in phase with 3.0 and 10 cps. A small counter-clockwise loop was added to the main clockwise one in a case with 10 cps; a small clockwise loop was added to the main counter-clockwise one once with 1.0 and once with 10 cps. Lags were the rule when higher frequencies, e.g., 50–100 cps, were examined.

The change with stimulus frequency of the shape of the rate vs. length graphs was illustrated by the composite from all experiments in Fig. 6: lengths and

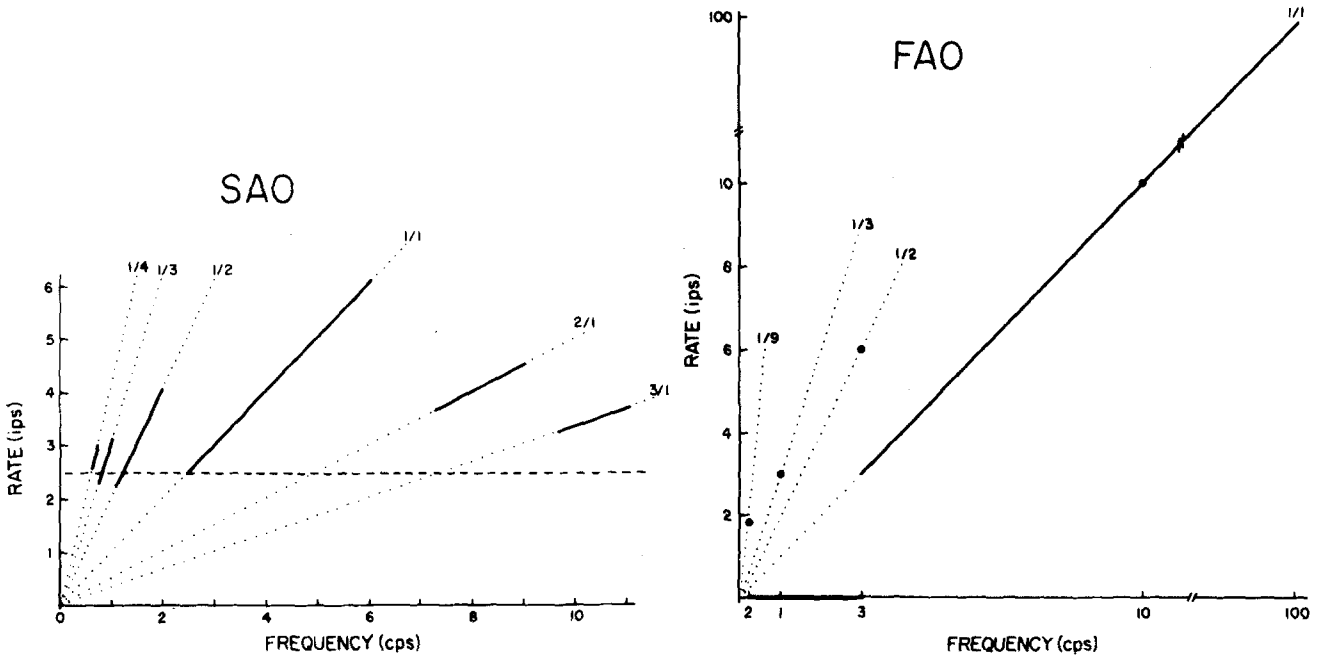

Fig. 3. Overall rate vs. stimulus frequency. On the abscissae and the ordinate corresponding stimulus frequencies and afferent overall rates, respectively, over a stationary period. The slopes are indicated by broken lines. *Left plot:* Slowly Adapting Organ (SAO). Modulation depth, 0.21 mm; spontaneous rate, 2.5 ips. There were interposed segments where patterns were unclear. 1/4, 1/3, 1/2, 1/1, 2/1, and 3/1 locking ratios (number of cycles/number of impulses) were observed. *Right plot:* Fast Adapting Organ (FAO). Modulation depth, 0.30 mm. The receptor did not discharge with frequencies below 3.0 cps, and locked 1/1 from 3.0 to 100 cps. Dots represent the overall average rates at the commonly studied frequencies from the same experiment from which the cycles in Fig. 1 were obtained. Average discharge fell in segments with locking ratios that were less than 1/1 with 0.2, 1.0, and 3.0 cps. With 10 cps, discharge rate fell in the 1/1 locked segment

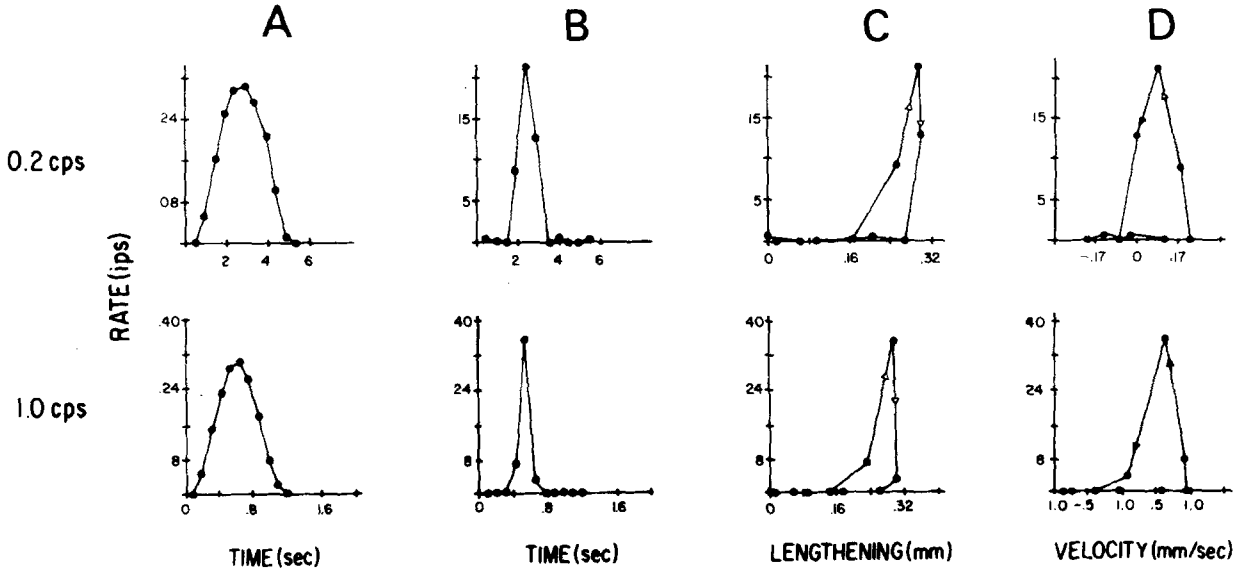

Fig. 4A–D. Length modulation with 0.2 and 1.0 cps. The following applies to Figs. 4 and 5. Abscissa time along the cycle (*s* or *ms*) in **A** and **B**, mean length (mm, zero at the minimum) in **C**, and velocity (mm/s) in **D**; ordinate mean length in **A**, mean afferent rate (ips) in **B–D**. **A**, average stimulus cycle; **B**, discharge rate cycle histogram; **C**, basic average Lissajous figure with length on the abscissa, and rate on the ordinate, both corresponding to the same particular part (bin) of the cycle. The order of generation of points was indicated by the arrows. **D**, average Lissajous of rate vs. velocity. The following applies only for Fig. 4: 0.2 cps: actual modulation frequency, 0.21 cps, period, 4.81 s (bin-width, 0.481 s); modulation depth, 0.30 mm, total receptor length, 4.8 mm; *N* of cycles averaged 17. 1.0 cps: actual modulation frequency, 0.93 cps; period, 1.08 s (bin-width, 0.108 s); modulation depth, 0.30 mm, total receptor length, 4.8 mm; *N*, 36

rates were expressed as percentages of the peak values in each case, allowing comparison of diverse depths. In general, the "openess" of the rate vs. length loops decreased with stimulus frequency. This implied also that, in general, double-valuedness became less marked. Local exceptions were clear, however: for example, when discharges locked out of phase (lag) at 30–100 cps, the separation of the two values became very large.

The "flat extension" with zero rates to the left includes bins during shortening and elongation. It coincides with the no-discharge period during lengthening in the majority of cases (clockwise loops, leads) because firing starts as length increases at a smaller length than that at which it stops during shortening; the flat extension coincides with the no-discharge period during shortening in the minority of cases (counter-clockwise loops). The rule in either case was that, when the stimulus frequency increased, the points where firing started during elongation and ceased during shortening occurred proportionately closer to where length was maximum, i.e., firing started later and stopped earlier: therefore, more of the cycle was silent and the flat extension longer. The percentage differences "silent period during shortening minus that during elongation" were positive for clockwise cases and negative for counter-clockwise ones (Table 2); differences decreased with stimulus frequency in the counter-clockwise cases. The portions with zero rates imply a lower-limit saturation-like phenomenon.

Stimulus and discharge are "locked" (Kohn et al., 1981) when the visual inspection of the records, and particularly cycle histograms with outstanding narrow peaks, indicate that practically in every cycle, or in every so many, one or more spikes occur at about the same phase. Locking of the one-to-one (1/1) type, i.e., one spike in every cycle, was present and evident to the naked eye in 13% (3 of 23 cases) with 3.0 cps and in

Table 1. Rates and number of spikes per cycle vs. stimulus frequency

	Depth (mm)	Stimulus frequency (cps)			
		0.2	1.0	3.0	10
Overall average rate (ips)		1.12	2.0	3.15	8.0
Average peak rate (ips)	0.09	12.44	22.22	35.0	88.9
Average number/cycle		5.6	3.15	1.01	0.8
		0	0	3.08	10.0
	0.12	0	0	25.7	83.3
		0	0	0.99	1.0
		1.05	3.4	6.09	10.0
	0.18	5.83	18.8	33.9	55.5
		5.30	3.4	2.07	1.0
		0	1.95	2.92	9.8
	0.21	0	9.29	13.90	46.7
		0	2.05	0.99	0.98
		1.72	2.0	6.0	10.4
	0.24	7.16	8.3	25.0	43.3
		8.6	2.0	2.04	1.04
		0	0	3.40	11.0
	0.30	0	0	14.17	36.7
		0	0	1.09	0.99
		1.03	2.4	3.81	5.59
	0.39	2.64	6.15	9.77	14.33
		4.95	2.52	1.28	0.56
		4.92	5.76	14.70	30.0
	0.75	6.56	7.7	19.6	40.0
		24.63	6.06	5.01	3.0

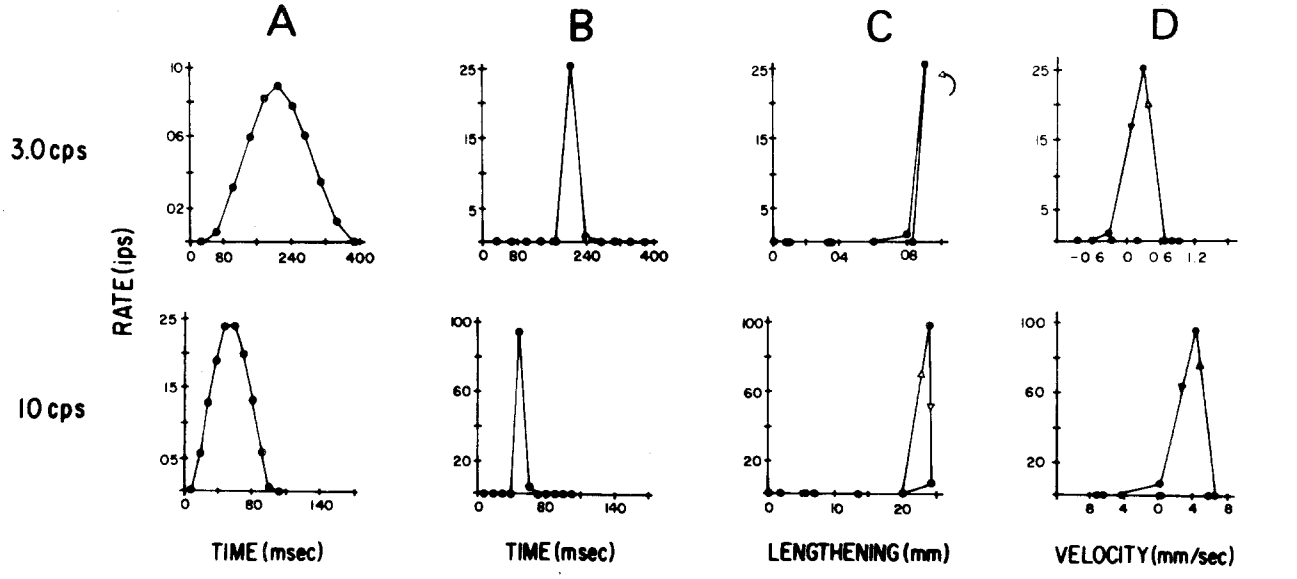

Fig. 5A–D. Length modulation with 3.0 and 10 cps: 3.0 cps: actual modulation frequency, 2.94 cps; period, 0.34 s (bin-width 0.034 s); modulation depth, 0.09 mm; receptor length, 4.8 mm (same receptor as in Fig. 4 with 0.2 cps); *N*, 145. 10 cps: actual modulation frequency, 10 cps; period, 0.1 s (bin-width, 0.01 s); modulation depth, 0.24 mm; *N*, 321

Table 2. Response characteristics and stimulus frequency

	0.2 cps	1.0 cps	3.0 cps	10 cps
Cases	19	17	23	17
Non-zero valued bins	9(5%)	–	–	–
	7(11%)	–	–	–
	6(5%)	–	–	–
	5 –	–	5(9%)	–
	4(16%)	4(6%)	–	–
	3(42%)	3(71%)	3(52%)	3(24%)
	2(21%)	2(18%)	2(26%)	2(41%)
	1 –	1(6%)	1(13%)	1(35%)
1-to-1 "locking"	0	0	3(13%)	6(35%)
Shut-off (% of period)	63%	75%	74%	82%
Clockwise loops	18(95%)	14(82%)	17(74%)	12(71%)
Lead	1 bin	1 bin	1 bin(76%) 2 bin(24%)	1 bin

** The calculations below were based upon 16, 14, 14, and 10 cases at 0.2, 1.0, 3.0, and 10 cps, respectively.

Silence during elongation (flat extension)				
% of depth	47%	56%	60%	71%
CV	0.54	0.24	0.21	0.23
Silence during shortening (discharges cease)				
% of depth	67%	89%	90%	92%
CV	0.40	0.07	0.06	0.11
Difference	20%	33%	30%	21%
CV	0.81	0.47	0.40	0.96
Counter-clockwise loops	1(5%)	3(18%)	5(22%) in phase	5(29%) in phase
Lag	2 bins	1 bin	(17.6%) 1 bin(4.4%)	(17.4%) 1 bin(11.6%)
Silence during elongation				
% of depth	100%	94%	81%	92%
CV	–	0.02	0.16	0.14
Silence during shortening (flat extension)				
% of depth	28%	38%	62%	79%
CV	–	0.05	0.35	0.12
Difference	−71%	−56%	−20%	−14%
CV	–	0	0.71	0.83

Table 3. Sensitivity and stimulus frequency

Bin width (ms)	Stimulus frequency (cps)			
	0.2	1.0	3.0	10.0
Modulation depth: 0.09 mm				
10	0–24 ips	0–61 ips	0–78 ips	0–80[a] ips
20	0–15	0–39	0–50[a]	0–45
50	0–10	0–20	0–20	0–30[a]
100	0–7.2	0–10[a]	0–10[a]	—
150	0–7.4	0–12[a]	0–6.5	—
300	0–6.7	0–10[a]	0–3.3	—
500	0–6.0[a]	0–4	—	—
Modulation depth: 0.075 mm				
10	0–45	0–100[a]	0–97	0–100[a]
20	0–45	0–50	0–74	0–100[a]
50	0–39	0–40	0–58[a]	0–40
100	0–37	0–32	0–38[a]	—
170	0–36[a]	0–24	0–19	—
350	0–31.5[a]	0–17	—	—
525	0–33[a]	1.9–9.4	—	—

[a] Highest sensitivity

35% (6/17) with 10 cps (Table 2). Locking was present also with 0.2 and 1.0 cps, but was less apparent, involving more spikes and less invariant ones. The usual bin-widths of 0.5 and 0.1 s were too large to reveal such locking: hence, the point was analyzed constructing histograms with numerous small bins. Figure 7, for example, is from a 1.0 cps case where at the larger elongations a burst of 5 or 6 spikes appeared in each cycle: the histogram (Fig. 7A) with 100 10-ms bins shows a succession of peaks separated by zero-valued troughs which reveal the tendency for discharges to occur in restricted portions of the cycle. The reduction and broadening of successive peaks indicated that the tendency decreased with succeeding spikes: the most, and the least, locked were the first, and the last, that occurred in the same bin in 88% (30/34), and in 23.5% (8/34), respectively. The between-cycle variability of the tallies (Fig. 7B) was low for bins with high or zero averages and high for those with intermediate ones: hence, the point along the burst where locking disappears depends on the boundary criterion selected for locking. The stimulus frequency ranges at which different locking ratios occurred were determined by background length and modulation depth, but this was not studied systematically.

Two types of average rate vs. velocity plots were common, both with counter-clockwise loops. The most common, corresponding to clockwise rate vs. length displays, had a flat extension to the left and a trapeze-like loop, with a peak to the right and the larger base on the abscissae (Figs. 4D and 5D): the discharge, absent as velocity augmented from zero to positive during the first half of the elongation, began near maximum positive velocity, peaked about halfway along the decreasing positive velocity, decayed, and then disappeared during the increasing negative velocity. An also common type, corresponding to 10 and sometimes 3 cps counter-clockwise rate vs. length loops, was a triangular loop peaking near zero velocity, and flat extensions on both sides (Fig. 5D).

The average rate vs. acceleration plots showed with all frequencies a right flat extension and a counter-clockwise triangular or trapeze-like loop peaking to the left. The cell did not discharge at maximum positive acceleration, began discharging near zero acceleration, peaked during the increasing negative, then

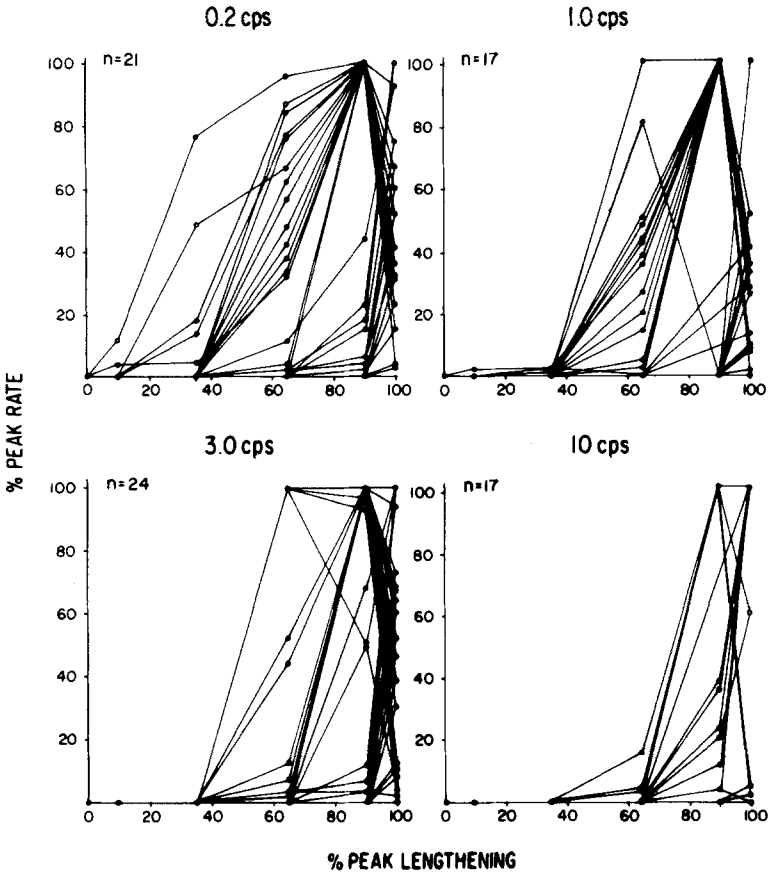

Fig. 6. Stimulus frequency and the shape of the rate vs. length plots. Length (abscissae) and rates (ordinates) were expressed as percentages of the peak values in each case, allowing comparison of diverse modulation depths. In general, the "openness" of the loops decreased with frequency

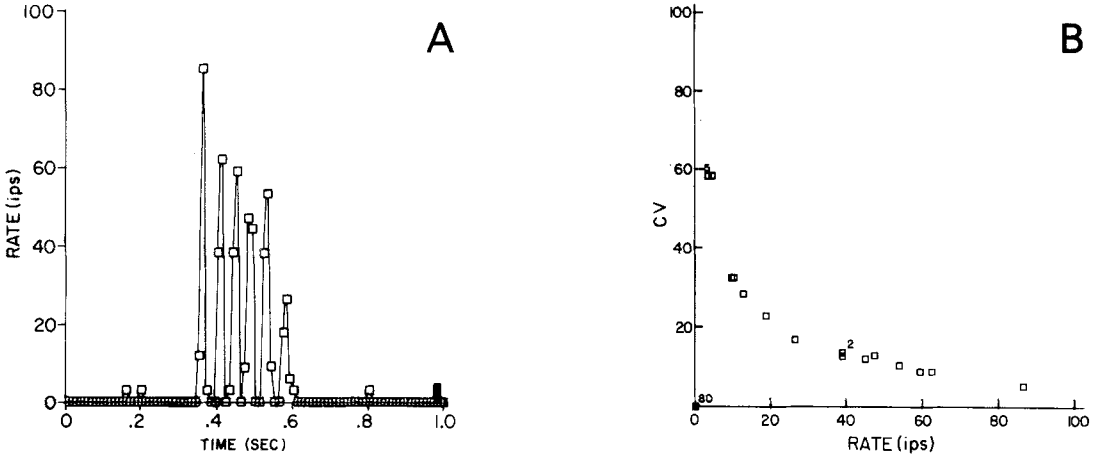

Fig. 7A and B. Locking with low frequencies. Length modulation at 1.0 cps. Actual modulation frequency, 1.02 cps; period, 0.98 s; (bin-width, 0.010 s); modulation depth, 0.27 mm; total receptor length, 4.95 mm; *N*, 34. **A** Cycle histogram: average discharge rate versus time along the cycle. **B** Coefficient of variation (CV) vs. time along the cycle

decayed and stopped during the decreasing negative accelerations.

The sensitivity to length was measured by the difference between the maximum and minimum bin rates in the cycle histogram at different frequencies with set background length (close to resting) and depth (e.g., 0.09 or 0.75 mm). Values for bin-widths between 10 and 500 ms and 0.09 and 0.75 mm depths are in Table 3. The minimum rate was zero always. For each frequency, as the bin-width increased, peak rates usually diminished, more markedly with the higher frequencies (Fig. 8). The highest sensitivity was dependent upon the bin-width chosen and the modulation depth. Using the shallower one (0.09 mm) it was highest with

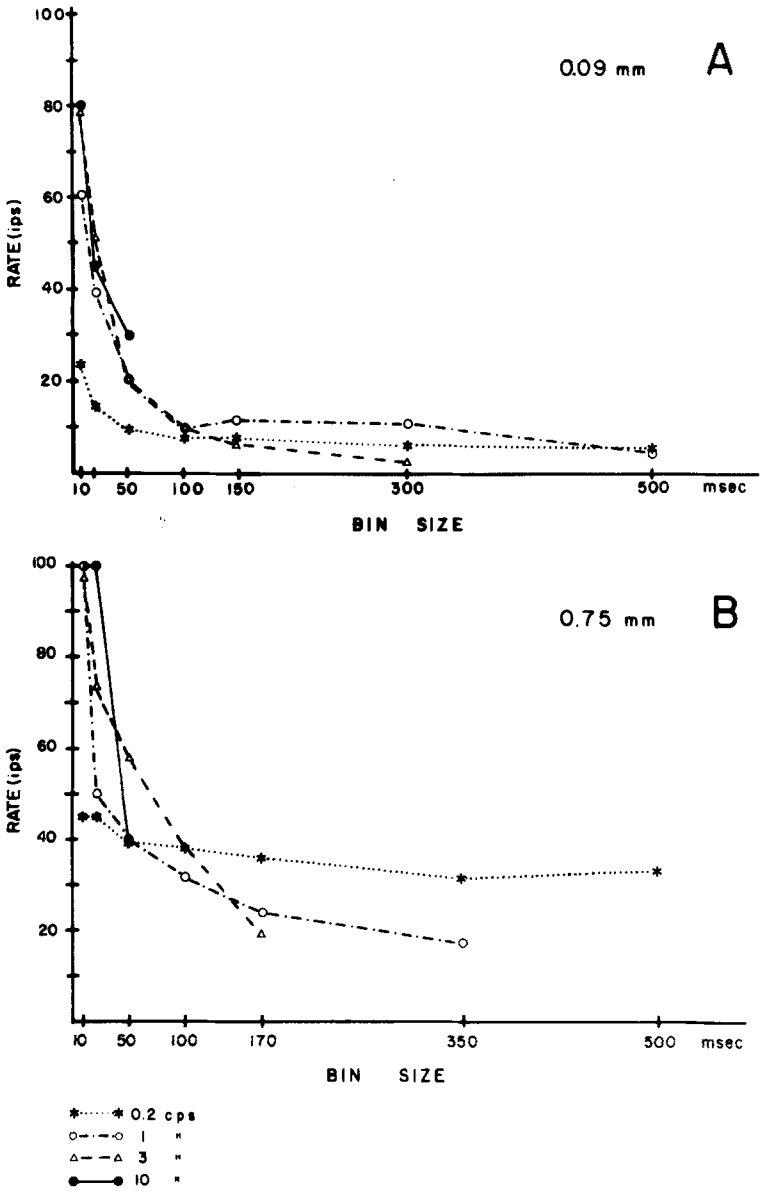

Fig. 8A and B. Overall sensitivity and effect of bin size. The difference between maximum and minimum bin rates in the average discharge was determined at different frequencies using 5000 spikes, and identical bin-widths. Bin-widths from 10 to 500 ms were used. **A** Modulation depth, 0.09 mm, receptor length, 11.7 mm; **B** Modulation depth, 0.75 mm, receptor length, 8.25 mm. Sensitivity was highest at high frequencies when using small bin-widths and with low frequencies using large ones

10 cps when using small bin-widths of 10 ms, with 1.0 cps when using intermediate ones up to 300 ms, and with 0.2 cps using 500 ms. Using 0.75 mm, sensitivity was highest with 1 and 10 cps with 10 ms, 10 cps with 20 ms, 3.0 cps with 50 and 100 ms, and 0.2 cps with larger bin-widths. The sensitivity to velocity varied during the cycle and was not symmetric around the zero velocity line. The sensitivity issue is discussed by Vibert and Segundo (1979).

The slowly adapting organ (SAO) was tested up to frequencies beyond the highest (5.0 cps) used so far (see Methods). When displayed as a function of stimulus frequency, the afferent overall rate showed alternating increasing and decreasing segments (Fig. 3). The increasing ones had 3/1, 2/1, 1/1, 1/2 slopes and exhibited locking (Fig. 9); the maximum afferent rate corresponded to the rightmost end of the 1/1 segment. Points in the decreasing segments had rate-to-frequency ratios such as exactly 2/5. The number of impulses per cycle decreased with frequency (e.g., 3 per cycle at 1.0 cps and 1 per cycle at 3.0 cps with 0.21 mm, Fig. 9); it increased at each frequency with increasing depths.

Discussion

The main point stressed here is the extreme complexity of sensory transduction in the FAO where characteristic stimulus distortions are pervasive, and can be ignored exclusively within unnaturally restricted operational domains. Indeed, during sinusoidal and within-natural-range stretchings, the afferent discharge modu-

lation was clearly non-sinusoidal, changing at different stimulus frequencies. Its general response description (Figs. 1, 3–5, and 7) holds also (though differing in some senses) for the SAO, mammalian muscle spindles (Grüsser and Thiele, 1968), and probably other receptors. The shared general features follow. i) The "afferent overall rate vs. stimulus frequency" graph was a zig-zag with broad segments having positive rational slopes, and narrow segments having overall negative slopes. Hence, linear theory interpretations based upon Bode plots are misleading. ii) The positively-sloped segments were continuous, and within them discharges and stimuli were locked. The "locking ratio" of numbers of cycles and impulses and its reciprocal, the slope, depended on the stimulus frequency: with low ones there were several impulses per cycle, early ones well-locked and late ones more variable; with intermediate frequencies, locking was 1/1; with high ones, impulses occurred regularly only once every several cycles. Higher frequencies, presumably contending with refractoriness and a maximum rate, are associated with a saturation-like horizontal graph. iii) Within the negatively-sloped segments details were unclear; less straightforward lockings (e.g., at 5/2 ratios) were sometimes present. iv) Non-linearities, i.e., saturation, asymmetric rate sensitivity and locking, were prominent and ubiquitous with periodic modulation, forcing their acceptance as major, commonplace transduction characteristics.

There are some SAO vs. FAO differences. The FAO does not discharge spontaneously or during slow modulations (Fig. 3), and therefore does not signal low frequencies (unless perturbed, Buño et al., 1978; Diez Martínez and Segundo, in preparation). Its 1/1 locking range is broad, e.g., 1–100 cps. Thus, though not active spontaneously, it oscillated when forced (Basar, 1976). The SAO, on the other hand, is a pacemaker, and stimulus frequencies can be referred to spontaneous ones. It responds to slow sinusoids (e.g., 0.3 cps, Brown and Stein, 1966; Chaplain et al., 1971), probably below those where the FAO starts responding, but rigorous comparisons are not available. The SAO 1/1 range is narrower, ending at about 3 cps: thus, it is less capable of a straightforward signaling of high frequencies.

Using few similar frequencies of sinusoidal stretch ($\sin \omega t$), the overall rate vs. frequency (ω) plot may appear linear, suggesting that receptors responded proportionately to stretch velocity ($\omega \cos \omega t$). Appearances would be misleading, however, because the graph is, at best, piece-wise linear, proportionality changing from one locked segment to the next, and the interposed segments being unclear.

Locking between interacting periodic variables derives from abstract concepts, not requiring particular physical attributes for explanation (Winfree, 1980):

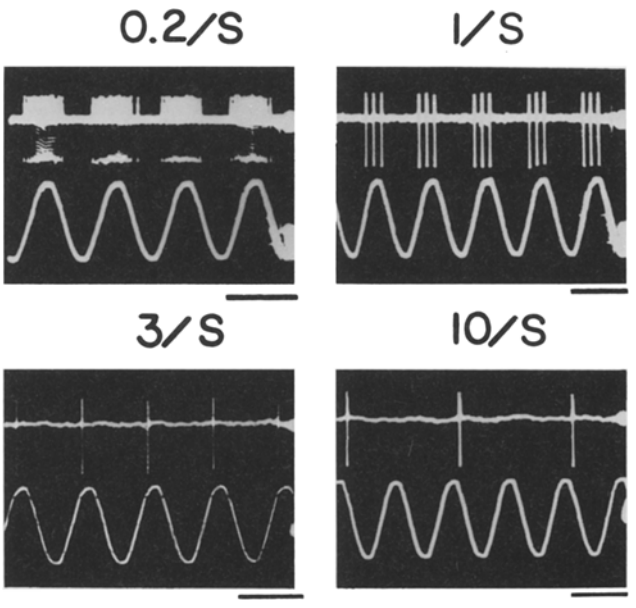

Fig. 9. Effect of stimulus frequency upon spike discharge in the slow adapting organ (SAO). Actual modulation frequencies, 0.198, 1.0, 2.94, and 10 cps; modulation depth, 0.21 mm. The spontaneous discharge rate for the 1-min period previous to each sinusoidal stimulation, 3.3 ips. Time calibrations, 5.05, 1.0, 0.34, and 0.10 s for 0.2, 1.0, 3.0, and 10 cps, respectively, identical to the cycle duration in each case. The number of spikes per cycle decreased as stimulus frequency increased. There were 15, 3, and 1 spikes per cycle with 0.2, 1.0, and 3.0 cps. With 10 cps there were no discharges in some cycles

examples abound among mechanoreceptors (e.g., Pringle and Wilson, 1952; Kiang, 1965; Talbot et al., 1968; Grüsser and Thiele, 1968). Neuronal models lock with applied current sinusoids. In the leaky integrator (Holden, 1976a; Stein et al., 1972), locking becomes less marked when, with the time-constant increasing, it approaches the perfect integrator that does not lock. In space-clamped patches of Hodgkin-Huxley membrances (Holden, 1976b), locking happens at intermediate frequencies, failing because of Na^+ inactivation predominance at low frequencies and insufficient time for Na^+ activation to develop at high ones. Particularly pertinent to mechanoreceptors is the electro-hydraulic excitability analog, an extension of an oscillator model (Teorell, 1959c, 1974, 1976, 1980). It considers the membrane's electro-chemical gradients and viscoelasticity, conceiving it as having charged and uncharged pores and a constant current source that supplies potential gradients: rhythmic, impulse-like fluctuations of potential and conductance occur, synchronized with solute-solvent displacements and with volume and transmembrane pressure changes. When the electrohydraulic analog was subjected to sinusoidal pressure variations (Teorell, 1959, 1966), low frequencies induced discharges only with large amplitudes, intermediate frequencies induced locked

impulses, and fast ones only small graded responses. The full-sized responses at intermediate frequencies imply "pararesonance" (Walter, 1959), a phenomenon whereby a forcing function acting upon an oscillator will produce the maximum discharge rate with least energy expense, i.e., most economically, if it is at the system's natural frequency: FAO 1/1 lockings could be pararesonances at rates where a potential pacemaker has the lowest threshold.

Lissajous loops imply double-valuedness for several lengths, with one rate for elongation and another for shortening, a finding perhaps more widespread than recognized in sensory reception. With increasing modulation frequency, their separation and the loop "openess" decreased, a trend that is exceptional and encountered only in current-voltage plots of incandescent and fluorescent lamps, contrary to the commonplace loop widening (Campbell et al., 1953; Francis, 1948). Yet another "historical" issue is the initial rate modulation reduction (Fig. 2), whereby identical length swings determine decaying discharge swings. Initial adjustment of the stress response in tissues subjected to cyclical strains is common, and called "preconditioning" (Fung, 1981): it may occur in the stretch receptor, and explain the initial drop. All this raises the question of how afferent discharges, determined by present and by previous conditions, can inform central mechanisms precisely about stimulus magnitude.

The FAO remained silent during much of the cycle (Figs. 4–6), in the lower-limit saturation distortion expected because of the impossibility of negative rate variations in a spontaneously silent, rapidly adapting receptor (Holden, 1976a). As a rule, saturation decreased with decreasing frequency (Table 2, Fig. 6) [and with increasing depth, or background length (Dietz Martínez and Segundo, in preparation)].

The "stimulus velocity-discharge rate" relation (Figs. 4 and 5) was non-linear: furthermore, the FAO shares with other mechanoreceptors the widespread property of assymetric rate sensitivity (Buño et al., 1978; Clynes, 1969; Vibert and Segundo, 1979), implicit in the classical finding that a silent FAO responds to a lengthening, but ignores subsequent shortenings if previously adapted to zero discharge (Eyzaguirre and Kuffler, 1955). Its advantages are discussed elsewhere (Vidal et al., 1971). The membrane oscillator model shows greater firing changes with rising than with falling pressure (Teorell, 1959). Receptors whose response to step lengthenings adapts completely are approximated by first-order lead systems and high-pass filters for sinusoids (Partridge, 1973): the gain increases below a critical frequency proportionately with the input frequency (i.e., its first derivative), and above it the gain is constant.

These length-discharge transduction facets may arise at any of the conversion stages. Most pertinent data refer to the mechanical "length to neuronal distortion" stage, and were collected in the SAO. Since sinusoidally stretched SAO's did not develop negative tensions below resting length, tension vs. length plots were half-ellipses: non-linearities were particularly obvious at low frequencies, and the half-ellipse "openess" tended to decrease with increasing stimulus frequency (Chaplain et al., 1971). This was modeled by a "non-linear spring" in parallel with a "dashpot-linear spring series": the non-linearity originates at low frequencies in both parallel spring and dashpot, and at high frequencies, where the dashpot is stiff, exclusively in the former. Length-tension plots suggest that the discharge is tension-related (Krnjevic and van Gelder, 1961; Wendler and Burkhardt, 1961), and could explain the rate vs. length loops (Brown and Stein, 1966; Chaplain et al., 1971; Vibert and Segundo, 1979): factors perhaps encoder-related (see above) cannot be excluded, however. Similar considerations may hold for the FAO, whose mechanical properties differ little from the SAO's (Krnjevic and van Gelder, 1960, 1961). The length-tension conversion does not suffice to explain FAO behavior, however, since silent portions occupy more than a half-cycle and increase with frequency. Furthermore, although the generator potential follows muscle tension better than length, the "tension-generator potential" relation is non-linear (Nakajima and Onodera, 1969b).

A mathematical model (Chua and Bass, 1972) of looping in externally-driven physical systems behaves qualitatively very much like the FAO or SAO. It involves a first-order non-linear differential equation that, with increasing stimulus frequency, shows loop widening, narrowing or invariance, depending on a piece-wise linear function W of stimulus velocity. The FAO-model similarity when certain W functions are used, and the difficulties in correlating W with the physiological realities, are discussed elsewhere (Diez Martínez and Segundo, in preparation).

References

Basar, E.: Biophysical and physiological systems analysis. Reading, MA: Addison-Wesley 1976

Borsellino, A., et al.: Transfer functions of the slowly adapting stretch receptor organ of Crustacea. Cold Spring Harbor Symp. Quant. Biol. **30**, 581–586 (1965)

Brown, M.C., Stein, R.B.: Quantitative studies on the slowly adapting stretch receptor of the crayfish. Kybernetik **3**, 175–185 (1966)

Brown, M.C.: Some effects of receptor muscle contraction on the response of slowly adapting abdominal stretch receptors of the crayfish. J. Exp. Biol. **46**, 445–458 (1967)

Buño, W., Jr., et al.: Crayfish stretch receptor organs: Effects of length-steps with and without perturbations. Biol. Cybern. **31**, 99–110 (1978)

Campbell, J.H., et al.: Characteristics and applications of high-frequency fluorescent lighting. Illum. Eng. **48**, 95–103 (1953)

Chaplain, R.A., et al.: Systems analysis of biological receptors. I. A quantitative description of the input-output characteristics of the slowly adapting stretch receptor of the crayfish. Kybernetik **9**, 85–95 (1971)

Chua, L.O., Bass, S.C.: A generalized hysteresis model. IEEE Trans. Circ. Theor. **19**, 36–48 (1972)

Clynes, M.: Rein control, or unidirectional rate sensitivity, a fundamental dynamic and organizing function in biology. Ann. N. Y. Acad. Sci. **156**, 627–968 (1969)

Eyzaguirre, C., Kuffler, S.W.: Processes of excitation in the dendrites and in the soma of single isolated sensory nerve cells of the lobster and crayfish. J. Gen. Physiol. **39**, 87–119 (1955)

Francis, V.J.: Fundamentals of discharge tube circuits. New York: Wiley 1948

Fung, Y.C.: Biomechanics. Mechanical properties of living tissues. Berlin, Heidelberg, New York: Springer 1981

Grüsser, O.J., Thiele, B.: Reaktionen primärer und sekundärer Muskelspindelafferenzen auf sinusförmige mechanische Reizung. I. Variation der Sinusfrequenz. Pflügers Arch. **300**, 161–184 (1968)

Holden, A.V.: Models of the stochastic activity of neurons. Berlin, Heidelberg, New York: Springer 1976

Holden, A.V.: The response of excitable membrane models to a cycle input. Biol. Cybern. **21**, 1–7 (1976)

Kendall, M.G.: Rank correlation methods. London: Griffin 1970

Kiang, Y.-S.N.: Discharge patterns of single fibers in the cat's auditory nerve. Cambridge, MA: MIT Press 1965

Kohn, A.F., et al.: Presynaptic irregularity and pacemaker inhibition. Biol. Cybern. **41**, 1–14 (1981)

Krnjevic, K., van Gelder, N.M.: The effects of stretch on the tension and rate of discharge of crayfish stretch receptors. J. Physiol. **154**, 27 (1960)

Krnjevic, K., van Gelder, N.M.: Tension changes in crayfish stretch receptors. J. Physiol. **159**, 310–325 (1961)

Nakajima, S., Onodera, K.: Adaptation of the generator potential in the crayfish stretch receptors under constant length and constant tension. J. Physiol. (London) **200**, 187–204 (1969)

Partridge, L.D.: Biological receptors. In: Engineering principles in physiology, Vol. I. Brown, J.H.U., Gann, D.S. (eds.). New York: Academic Press 1973

Pringle, J.W.S., Wilson, V.J.: The response of a sense organ to a harmonic stimulus. J. Exp. Biol. **29**, 220–234 (1952)

Stein, R.B., et al.: The frequency response, coherence and information capacity of two neuronal models. Biophys. J. **12**, 295–322 (1972)

Talbot, W.H., et al.: The sense of flutter-vibration: Comparison of the human capacity with response patterns of mechanoreceptive afferents from the monkey hand. J. Neurophysiol. **31**, 301–334 (1968)

Teorell, T.: Biophysical aspects on mechanical stimulation of excitable tissues. Acta Soc. Med. Ups. **64**, 341–352 (1959c)

Teorell, T.: Electrokinetic considerations of mechanoelectrical transduction. Ann. N. Y. Acad. Sci. **137**, 950–966 (1966)

Teorell, T.: A biophysical formalism of the electromechanical events of the heart. In: Actualités neurophysiologiques. Monnier, A. (ed.). Paris: Masson 1974

Teorell, T.: Non-linear transport and oscillations in fixed charge membranes: some possible biological implications. In: Charged gels and membranes, Part I. Sélégny, E. (ed.). Dordrecht: Reidel 1976

Teorell, T.: A fixed charge system as a formal model for the behaviour of smooth muscles and the heart. Upsala J. Med. Sci. **85**, 201–209 (1980)

Vibert, J.F., Segundo, J.P.: Slowly adapting receptor organs: periodic stimulation with and without perturbations. Biol. Cybern. **33**, 81–95 (1979)

Vidal, J., et al.: Static and dynamic properties of gravity-sensitive receptors in the cat vestibular system. Kybernetik **9**, 205–215 (1971)

Walter, W.G.: Intrinsic rhythms of the brain. In: Handbook of physiology. Field, J. (ed. in chief), Sect. 1, Neurophysiology, Vol. I. Magoun, H.W. (section ed.). Washington, DC: American Physiological Society 1959, Chap. XI

Wendler, L.V., Burkhardt, D.: Zeitlich abklingende Vorgänge in der Wirkungskette zwischen Reiz und Erregung (Versuche an den abdominalen Streckreceptoren dekapoder Krebse). Z. Naturforsch. **166**, 464–469 (1961)

Winfree, A.T.: The geometry of biological time. Berlin, Heidelberg, New York: Springer 1980

Received: April 26, 1983

Oscar Diez Martínez
Departamento de Fisiología
Fac. de Medicina, UNAM
Aptdo. 70250 CU
México DF 04510
México